PCCP

Selective formation of molecular junctions with high and low conductance states by tuning the velocity of electrode displacement

Journal:	*Physical Chemistry Chemical Physics*
Manuscript ID	CP-ART-11-2019-006487.R1
Article Type:	Paper
Date Submitted by the Author:	27-Jan-2020

Complete List of Authors:	Isshiki, Yuji; Tokyo Institute of Technology, Department of Chemistry Fujii, Shintaro; Tokyo Inst. of Tech., Chemistry Nishino, Tomoaki; Tokyo Institute of Technology, Department of Chemistry Kiguchi, Manabu; Tokyo Institute of Technology, Department of Chemistry

ARTICLE

Selective formation of molecular junctions with high and low conductance states by tuning the velocity of electrode displacement

received 00th January 20xx,
Accepted 00th January 20xx

DOI: 10.1039/x0xx00000x

www.rsc.org/

Yuji Isshiki,[a] Shintaro Fujii,[a*] Tomoaki Nishino[a] and Manabu Kiguchi[a]

A single-molecule junction of 1,4-di(4-pyridyl)benzene (DPB) was prepared in a nano-gap between two Au electrodes using the scanning tunnelling microscopy-based break junction method (STM-BJ). Electric conductance and current versus bias voltage (*I*–*V*) measurements during the pulling and pushing processes of DPB single-molecule junctions revealed that high (H) and low (L) conductance states formed in the both pulling and pushing processes. Analysis of the *I*–*V* curves based on a single-level model indicated that the difference in conductivity of the H and L states mainly arises from high and low metal-molecule electric coupling in the junction. We demonstrated the controllable formation of H and L conductance states by simply tuning the velocity of electrode displacement in the pushing process. In the pulling process, both H and L states formed regardless the velocity (*v*) of electrode displacement, while in the pushing process, H and L states could be selectively fabricated by using low (*v* = 16 nm/s) and high (*v* = 64 nm/s) velocity of displacement, respectively. This study provides a simple approach to selectively fabricate high and low conductance states by fine tuning of electrode displacement.

Introduction

The understanding of charge transport through a single molecule plays an important role in building ultra-small electronic devices.[1-5] To measure the charge transport through a single molecule connected to two metal electrodes, nanofabrication methods of mechanically controllable break junctions (MCBJ) and scanning-tunnelling microscope-based break junctions (STM-BJ) have been developed.[6-8] In the BJ methods, a nano-gap is prepared by breaking a metallic point contact, and a single-molecule junction is fabricated by trapping a single molecule into the nanogap of the metal electrodes. Until now, by mechanically tuning the displacement of the electrodes, the ability to control modulation or switching of single-molecule conductance has been demonstrated. [4, 9-12] Quek *et al*. [10] and Taniguchi[9], Kim[11] *et al*. showed reversible binary switching in single-molecule conductance by mechanically oscillating an electrode and inducing switching between two metal-molecule interface structures for 4,4'-bipyridine[10] and 1,6-hexaneditiol.[11] Bruot *et al*. demonstrated that the orbital energy level(s) of a 1,4-benzenedithiol junction can be modulated by mechanically pulling and pushing the junction using a moving electrode.[12] Su *et al*. were able to mechanically switch conformational states with low and high electric conductance for single-molecule junctions of oligosilanes.[4] Most of the previous studies focused on trying to modulate the switching behaviours or the electronic states of single-molecule junctions with high and low electric conductance in response to mechanical perturbation.

Here, we focus on the selective fabrication of single-molecule junctions with high and low electric conductance and report a facile mechanical approach for controlled formation of high and low conductance states by simply tuning the velocity of electrode displacement in the junction. In this study, a single-molecule junction of 1,4-di(4-pyridyl)benzene (DPB) sandwiched between a pair of Au electrodes was fabricated using the STM-BJ method. The DPB single-molecule junction showed high (H) and low (L) conductance states during both pulling and pushing of the junction. We demonstrated that the H and L states can be selectively fabricated using low- or high velocity electrode displacements during the pushing process, while both H and L states formed independently of the velocity of electrode displacement during the pulling process.

Experimental section

Ethanol (as the solvent) and 1,4-di(4-pyridyl)benzene (DPB) were purchased from Kanto Chemical Co., Inc. and Tokyo Chemical Industry Co., Ltd., Japan, respectively. The Au(111) substrate was prepared by thermal deposition of Au (Tanaka Kikinzoku Kougyou K.K., Japan, purity >99.99%) on mica at 575 K under high vacuum. A sample was prepared by dipping the Au substrate into a 10 mM DPB ethanol solution. For the current measurements, we used a scanning tunnelling microscope (STM) (Nanoscope V, Bruker, Santa Barbara, CA) operating in air. A current amplifier with gain of 10 nA/V was used. The STM

Department of Chemistry, Graduate School of Science and Engineering, Tokyo Institute of Technology, 2-12-1 W4-10 Ookayama, Meguro-ku, Tokyo 152-8551,
E-mail: *fujii.s.af@m.titech.ac.jp*

tip was prepared by mechanically cutting a Au wire (Nilaco, Japan, diameter ≈ 0.3 mm, purity >99 %).

Single-molecule junctions were prepared using the STM-BJ method as described previously.[8,13,14] Briefly, the electric current through the junctions was monitored at a fixed bias voltage of 100 mV during the pulling and pushing modes of the junction (Fig 1a–c). The STM-BJ conductance measurement was performed with a signal access module (SAM III, Bruker, Santa Barbara, CA), a piezo driver (E-663 LVPZT-Amplifier, Physik Instrumente, Auburn, MA) and a data-acquisition-device (NI PXI-4461, National Instruments, Austin, TX).

I–*V* measurements of the single-molecule junction were conducted as follows: First, a Au point contact (< 10 G_0, $G_0 = 2e^2/h$, where G_0 is the quantum conductance) was made between the STM tip and the sample surface. Second, the tip was pulled by 5 nm at a speed of *ca*. 40 nm/s to break the Au contact and create a nanogap between the Au electrodes forming the molecular junction, during current monitoring at a fixed bias voltage of 20 mV. Third, the tip position was fixed, and a *I*–*V* curve was recorded (Fig. 1c). Finally, the tip was pulled by 15 nm to break the molecular junction in the pulling process. In a similar manner, a Au point contact (< 10 G_0, $G_0 = 2e^2/h$) was made between the STM tip and the sample surface in the pushing process. The tip was then pulled by 20 nm to break the Au contact and create a molecular junction. Next, the tip was pushed to the sample surface by 15 nm, and the tip position was fixed. Last, a *I*–*V* curve was recorded in the same way as described for the pulling process (Fig. 1e).

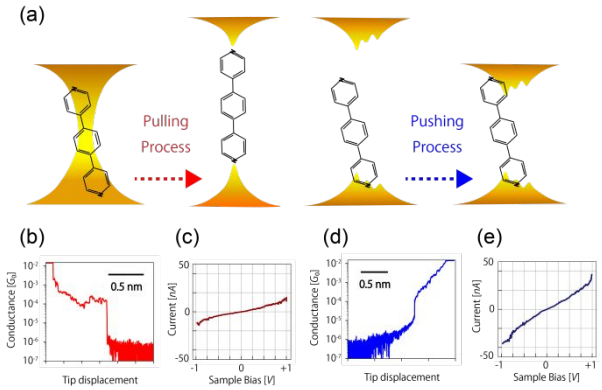

Fig. 1. (a) Structures of a 1,4-di(4-pyridyl)benzene junction. Red and blue arrows show the pulling and pushing processes of the junction, respectively. (b,d) Examples of conductance traces at 100 mV (b) in pulling and (c) pushing processes. (c,e) Example of *I*–*V* curves (c) in the pulling and (e) pushing process.

Results and discussion

1. Conductance versus tip displacement curve

The results of DPB-single-molecule conductance measurements are shown in Fig. 2. More than ten thousand conductance versus tip displacement curves of the single-molecule junction were measured, and were compiled into two-dimensional (2D) maps (Fig. 2a,b). The distributions in these maps were characterized by curved and linear distributions at the shorter tip displacement employed (<1 nm) during the pulling and pushing processes. To analyse the distributions, probable tip displacements were plotted as a function of logarithmically binned conductance. For example, the insets of Fig. 2a,b show displacement histograms within conductance ranges of (a) $10^{-3.91 \pm 0.01}$ G_0 and (b) $10^{-3.21 \pm 0.01}$ G_0 for the pulling and pushing processes, respectively. In the pulling process, the displacement histogram showed one Gaussian peak, while the pushing process was characterized by two Gaussian peaks. The analysis of the displacement histograms was performed for a conductance range from $10^{-4.0}$ to $10^{-2.0}$ G_0 with a bin size of 0.0162 nm for the pulling process and 0.0324 nm for the pushing process, and every probable displacement was determined by a Gaussian peak in the distribution (Figs. S1–S4 and Table S1). Fig. 2c,d shows plots of the probable tip displacements (*i.e.*, the Gaussian peak-positions in the displacement histograms) as a function of logarithmically binned conductance. The analysis of the probable displacements suggested that, in the pulling process, a conductance state with a *G* slope of a small absolute value ($d\log G/dz = -1.0$ nm^{-1}, where *G* is the conductance and *z* is the displacement) is likely to change to another state with a *G* slope ($d\log G/dz = -2.5$ nm^{-1}) of a large absolute value for small tip displacements (z < 0.2 nm, see Fig. 2c). In contrast, two independent conductance states with exponential displacement dependence are present in the pushing process (Fig. 2d).

To determine the probable single-molecule conductance values of DPB, conductance histograms were constructed from the conductance versus displacement curves (Fig. 2a,b), not considering the displacement values. Fig. 2e and Fig. 2f show the conductance histograms for the pulling and pushing process, respectively. Each conductance histogram was filled by two Gaussian distributions (Supplementary information 1), because the analysis of the probable displacements (Fig. 2c,d) suggests that two conductance states are present in both the pushing and pulling processes. Table 1 summarizes the results of the histogram fitting, in which the peak maxima were determined to be 0.16 and 0.26 mG_0 for the low (L) and high (H) conductance states in the pulling process, respectively, and 0.65 and 1.0 mG_0 for L and H states in the pushing process, respectively. The conductance of DPB in the pulling process is in good agreement with the single-molecule conductance of 0.21 mG_0 reported previously.[15]

2. Current-voltage characteristics

Fig. 3a,b shows 2D histograms of the *I*–*V* curves of DPB, which were built from more than four thousand *I*–*V* curves measured for pulling and pushing processes (Fig. S4). In the single-level model, *I*–*V* characteristic of a single-molecule junction can be represented by equation (1) (Figs. S5 and S6, Table S2, and Supplementary information 2).[13,16,17]

$$I(V) = \frac{8e}{h}\alpha(1-\alpha)\Gamma\left\{\tan^{-1}\left[\frac{\alpha eV-\varepsilon}{\Gamma}\right]+\tan^{-1}\left[\frac{(1-\alpha)eV+\varepsilon}{\Gamma}\right]\right\},$$

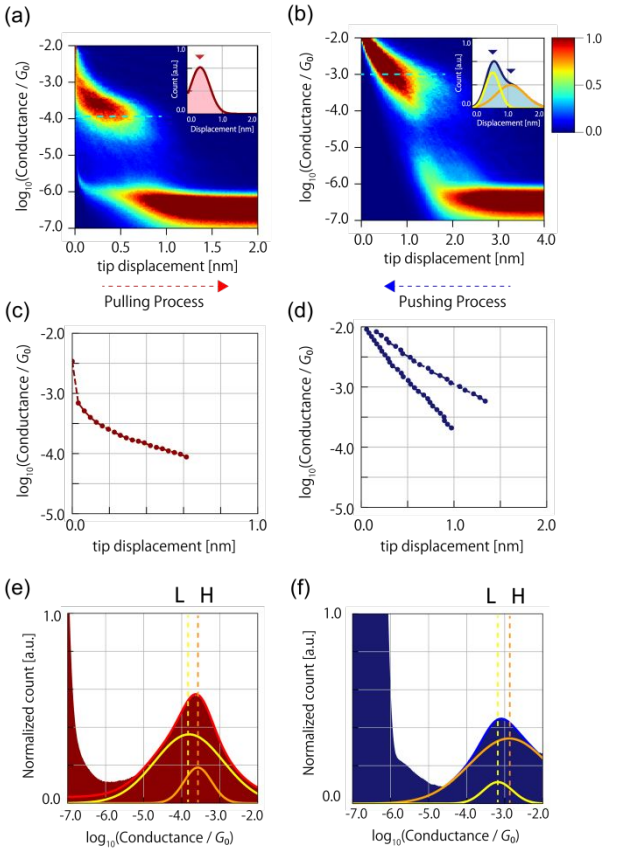

Fig. 2. (a,b) Two-dimensional (2D) histograms of conductance versus tip displacement curves measured during (a) pulling and (b) pushing processes of the junctions at the bias voltage of 100 mV. Linear *x*-bin sizes of 0.0162 nm for (a) and 0.0324 nm for (b) were used. The log-scaled *y*-bin size of $\Delta\log(G/G_0)$ was 0.0202 for both (a) and (b). Each 2D histogram was built from 12,359 conductance traces. We defined the tip displacement as the displacement from the tip position at the conductance of 0.014 G_0. Insets are histograms of tip displacement at the conductance of (a) $10^{-3.91\pm0.01}$ G_0 and (b) $10^{-3.21\pm0.01}$ G_0. The linear bin size is 0.0162 nm. (c,d) Plots of conductance versus probable tip displacement constructed from the data in (a) and (b). The probable tip displacements within certain conductance ranges ($\log(\Delta G/G_0)$ = 0.0202) were obtained as Gaussian peaks in the displacement histograms (For instance, see insets in (a) and (b)). In (b), the displacement histogram shows two Gaussian peaks, and two probable displacements were plotted for each conductance window. (e,f) Conductance histograms for (e) pulling and (f) pushing processes, which are compiled using that data in (a) and (b). A log-scaled bin size of $\Delta\log(G/G_0)$ = 0.0167 was used. Each histogram was fitted with double-Gaussian curves. The fitted results are indicated by the yellow and orange curves (*i.e.*, high (H) and low (L) states, respectively).

Equation (1)

where $\Gamma = \Gamma_R + \Gamma_L$, $\alpha = \Gamma_R/\Gamma$.

Here, ε represents the energy difference between the Fermi level of the electrode and the resonance level of the molecule, and $\Gamma_{R(L)}$ represents the electric coupling between the molecule and the right (left) electrode. Each measured *I*–*V* curve in both pulling and pushing modes (Fig. 3a,b) was fitted with equation (1), and the ε and Γ values were determined. We found that in all cases, the parameter α was almost 0.5 (*i.e.*, $\Gamma_L = \Gamma_R$) (Fig. S8), and therefore, in the analysis and discussion on the metal–molecule electric coupling in the following sections, we implicitly consider that $\Gamma = \Gamma_L + \Gamma_R$. Fig. 3c-f shows histograms of ε and Γ values. The histograms were fitted by two Gaussian distributions, because the analysis of the conductance versus tip displacement curves (Fig. 2) revealed that two conductance states are present during the pulling and pushing processes. The summary of this fitting is presented in Table 1. For both pulling and pushing processes, the H states show larger Γ and ε values compared to those of the L states. This result indicates that the higher conductance of the H states arises from the larger metal-molecule electric coupling Γ, since zero bias conductance can be described as $T(E=0) = \Gamma^2/(\Gamma^2+\varepsilon^2)$ (Supplementary information 2). In general, molecular orientation, rotation, substrate morphology such as (100) and (111), or stepped surface could potentially influence the molecular junction-conductance. For pyridine-based analogue molecules such as bipyridine and pyridine show H and L states depending on the molecular orientation in the junctions, and the H state can transform into the L state during pulling of the respective junctions.[10,13] This conductance behaviour is quite similar to that of the pyridine-based DPB studied here. In the H state of the pyridine-based analogue molecules, the molecule has a tilted orientation and the π-electrons in the pyridine ring can form π-type bonds with the Au electrode,[10,13,18] which results in large metal-molecule electronic coupling (Γ). In contrast, in the L state, the molecule has an upright orientation and the lone pair of the N atom forms σ-type N-Au bonding with low metal-molecule electronic coupling (Γ).

In contrast to the pulling process, in which the H state of DPB can transform to the L state along with the displacement of the electrode, the H and L states of DPB independently formed in the pushing process (Fig. 2d). Analysis in the *I*–*V* curves of DPB in the pushing process revealed that the H and L states showed similar ε (ε = 1.0 and 0.9 eV (Table 1)). These results suggested that two independent metal-molecule interface structures with substantial differences in electric coupling (Γ = 23 and 13 meV (Table 1)) formed in the pushing process of DPB.

3. Selective fabrication of the high and low conductance states

To obtain further insight into the nature of the observed H and L states, the conductance behaviour of our junctions was studied using various velocities (*v*) of tip displacement (*v* = 16, 32, and 64 nm/s) (Fig. S9). Fig. 4 shows 2D histograms of the conductance versus tip displacement curves for the pulling and pushing processes, measured at the velocity of 64 nm/s. By comparing the results obtained at *v* = 16 nm/s (Fig. 2a,b) with the 2D histograms at *v* = 64 nm/s (Fig. 4c,d), one can see that the conductance behaviour is obviously dependent on the velocity in the pushing process (Figs. 2b and 4d), while the conductance behaviour is almost independent on the velocity in the pulling process (Figs. 2a and 4c). Fig. 5a,b shows conductance histograms constructed from the data measured at *v* = 16 and 64 nm/s. The shape of the conductance histograms in the pushing process is apparently dependent on the velocity (Fig. 5b), which is in contrast to those in the pulling process (Fig. 5a). With the same procedure adopted in the conductance analysis in Fig. 2e,f, the histograms were fitted by two Gaussian

distributions, corresponding to the H and L states (Fig. S10). In the pulling process, the areas of the two Gaussian distributions (*i.e.*, the H and L states) remained almost constant regardless of the operation of different velocities of tip displacement (Fig. S10 and Table 2). In sharp contrast, the Gaussian area of the H state became *ca*. 1.9 times smaller at v = 64 nm/s compared to that at v = 16 nm/s in the pushing process (Fig. 5c,d). In this mode, the ratio of the areas of the Gaussian curves representing the H state relative to the L state is 0.3 at v = 16 nm/s, while the area ratio is 1.1 at v = 64 nm/s (Fig. 5e). This result indicates that one of the two conductance states in the pulling process can selectively form by tuning the velocity of tip displacement.

In a similar manner to the case of the pulling process, in pushing mode, H and L sates can arise from difference in the metal-molecule bonding, such the as σ- and π- bonding types described above (Figs. S11 and S12, Supplementary information 3). In contrast to the pulling process, one of the two ends of the molecule is free from bonds in the pushing process (Fig. 1a), and structural relaxation at the interface between the molecule and the Au surface can play a role in junction formation in the pushing process. For example, the diffusion constant of Au atoms on Au surfaces is around 0.9 nm^2/s at 300 K, according to a previous report,[19] which means that during a typical tip displacement of the order of 1 nm at v = 16 nm/s, Au atoms at the metal-molecule interface can diffuse on a surface of *ca*. 0.056 nm^2 (= 0.237 nm × 0.237 nm). This scale is comparable to the size of one Au atom (ca. 0.3 nm). Therefore, lower velocities we investigated, the metal-molecule interface structure can be subject to relaxation, which can cause change in the single-molecule conductance.

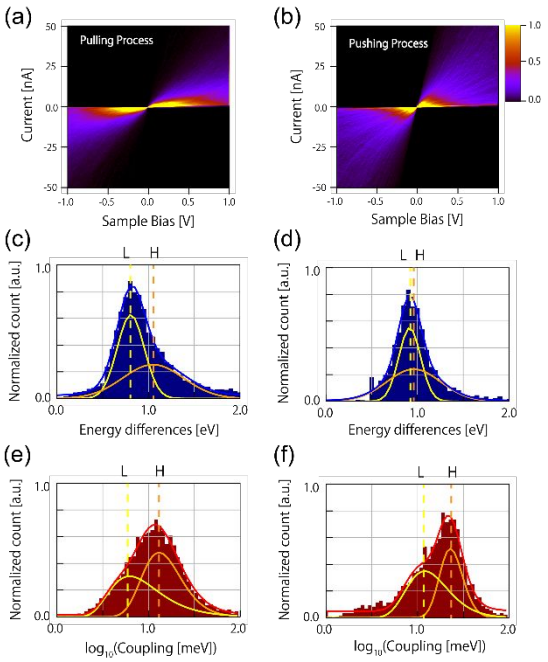

Fig. 3. (a,b) 2D mapping of the *I-V* curves of the DPB-single-molecule junction during the pulling and pushing processes, which were constructed from 6983 and 4064 *I-V* curves, respectively. A linear x bin size of 7.81 mV and a linear y bin size 0.391 nA are used. (c-f) Histograms of the energy differences (E_0) and the electronic coupling (Γ) in the pulling process (c,d) and the pushing process (e,f). A linear bin size of 0.05 eV is used for (c,e) A logarithmic bin size ($\Delta\log(\Gamma)$) of 0.04 is used for (d,f). The yellow and orange Gaussian curves correspond to the L and H states, respectively. Blue and red lines are the total Gaussian curve.

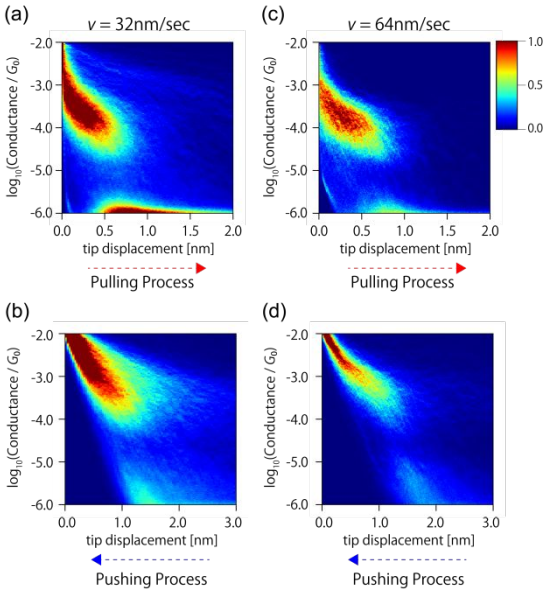

Fig. 4. 2D histograms of the conductance versus tip displacement curves measured at velocities of tip displacement (v) of (a,b) v = 16nm/s and (c,d) v = 64 nm/s. The histograms in (a,c) and (b,d) correspond to the pulling and pushing processes, respectively. A linear x bin size of 0.0162 and 0.0324 nm was used for (a,c) and (b,d), respectively. A log-scaled y bin size of $\Delta\log(G/G_0)$ = 0.0202 was used for (a-d).

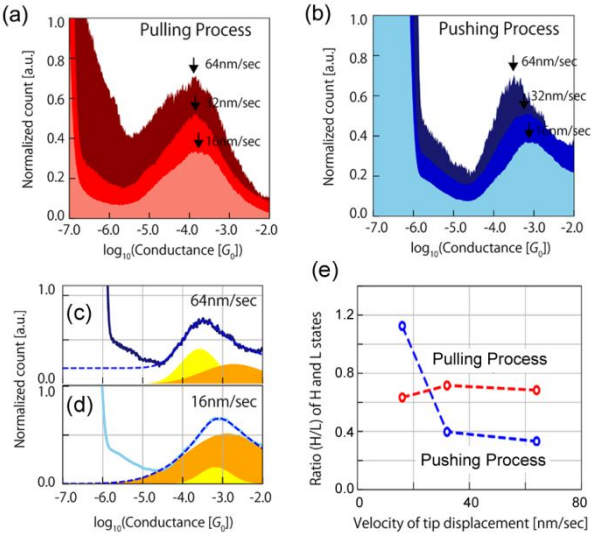

Fig. 5. (a,b) Conductance histograms constructed from data measured at different velocities (v) of tip displacement (v = 16, 32, and 64 nm/s) in pulling and pushing processes of the junction. Black arrows show the most probable conductance value in each case. (c,d) Conductance histograms in the pushing process, which were fitted with double Gaussian curves for v = 16 and 64 nm/s. Orange- and yellow-coloured Gaussian distributions correspond to the H and L states, respectively. (e) The Gaussian area ratio of the H state relative to the L state is plotted as a function of the velocity of tip displacement (see also Fig. S10).

Conclusions

In summary, we revealed the single-molecule conductance states of DPB in the pulling and pushing processes of a junction built using the STM-BJ method. Two states with high and low electric conductance were identified for both processes. The high conductance state predominantly formed in the pulling process. In contrast, the high conductance state in the pushing process was selectively fabricated when the velocity of tip displacement was fast. This study reports a simple mechanical approach to tune single-molecule conductance.

Process	State	G/mG_0	ε/eV	Γ/meV	α
Pulling	H	0.26	1.1	14	0.5
	L	0.16	0.8	8	0.5
Pushing	H	1.00	1.0	23	0.5
	L	0.65	0.9	13	0.5

Table 1. List of conductance, ε, Γ, and α values of the H and L states for pulling and pushing processes. Each value was determined from the peaks in the histograms of Fig. 2e,f and Fig. 3c–f.

	16 nm/s	32 nm/s	64 nm/s
Pulling	0.63	0.72	0.68
Pushing	1.13	0.74	0.33

Table 2. List of Gaussian area ratios of the H state relative to the L state represented (see Fig. 5 and Fig. S10).

Conflicts of interest

There are no conflicts to declare.

Acknowledgements

This work was financially supported by Grants-in-Aids for Scientific Research (Nos. 17K1910, 18H03896), JST CREST (No. JP-MJCR18I4), and JSPS Fellows: 19J21186 from MEXT Japan, and Tokyo Ohka, TEPCO memorial, REFEC, Yazaki Memorial, REFOST, and Hitachi metals foundation.

References

1. B. Capozzi, J. L. Xia, O. Adak, E. J. Dell, Z. F. Liu, J. C. Taylor, J. B. Neaton, L. M. Campos and L. Venkataraman, *Nature Nanotechnology*, 2015, **10**, 522–527.
2. S. Fujii, M. Ziatdinov, S. Higashibayashi, H. Sakurai and M. Kiguchi, *J. Am. Chem. Soc.*, 2016, **138**, 12142–12149.
3. R. Hayakawa, M. A. Karimi, J. Wolf, T. Huhn, M. S. Zollner, C. Herrmann and E. Scheer, *Nano. Lett.*, 2016, **16**, 4960–4967.
4. T. A. Su, H. Li, M. L. Steigerwald, L. Venkataraman and C. Nuckolls, *Nat. Chem.*, 2015, **7**, 215–220.
5. X. Yin, Y. Zang, L. Zhu, J. Z. Low, Z. F. Liu, J. Cui, J. B. Neaton, L. Venkaaraman and L. M. Campos, *Sci. Adv.*, 2017, **3**, eaao2615.
6. C. J. Muller, J. M. Vanruitenbeek and L. J. Dejongh, *Phys. Rev. Lett.*, 1992, **69**, 140–143.
7. J. M. van Ruitenbeek, A. Alvarez, I. Pineyro, C. Grahmann, P. Joyez, M. H. Devoret, D. Esteve and C. Urbina, *Rev. Sci. Instrum.*, 1996, **67**, 108–111.
8. B. Xu and N. J. Tao, *Science*, 2003, **301**, 1221–1223.
9. M. Taniguchi, M. Tsutsui, K. Yokota and T. Kawai, *Chem. Sci.*, 2010, **1**, 247.
10. S. Y. Quek, M. Kamenetska, M. L. Steigerwald, H. J. Choi, S. G. Louie, M. S. Hybertsen, J. B. Neaton and L. Venkataraman, *Nat. Nanotech.*, 2009, **4**, 230–234.
11. Y. H. Kim, H. S. Kim, J. Lee, M. Tsutsui and T. Kawai, *J .Am .Chem. Soc.*, 2017, **139**, 8286–8294.
12. C. Bruot, J. Hihath and N. Tao, *Nat. Nanotech.*, 2011, **7**, 35–40.
13. Y. Isshiki, S. Fujii, T. Nishino and M. Kiguchi, *J. Am. Chem. Soc.*, 2018, **140**, 3760–3767.
14. Y. Komoto, Y. Isshiki, S. Fujii, T. Nishino and M. Kiguchi, *Chem. Asian J.*, 2017, **12**, 440–445.
15. A. Borges, E.-D. Fung, F. Ng, L. Venkataraman and G. C. Solomo, *J. Phys. Chem. Lett.*, 2016, **7**, 4825–4829.
16. Y. Komoto, S. Fujii, H. Nakamura, T. Tada, T. Nishino and M. Kiguchi, *Sci. Rep.*, 2016, **6**, 26606.
17. R. Frisenda, Perrin, M. L., Valkenier, H., Hummelen, J. C. & van der Zant, H. S. J., *Phys. Status Solidi B*, 2013, **250**, 2431–2436.
18. T. Wandlowski, K. Ataka and D. Mayer, *Langmuir*, 2002, **18**, 4331–4341.
19. H. Göbel and P. von Blanckenhagen, *Surf. Sci.*, 1995, **331**–**333**, 885–890.

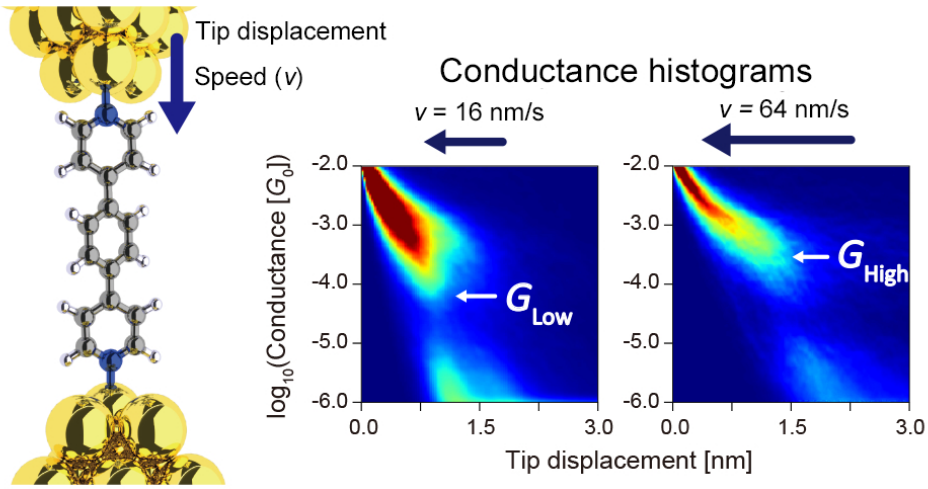
Tip displacement
Speed (v)
Conductance histograms
v = 16 nm/s
v = 64 nm/s
log10(Conductance [G0])
-2.0
-3.0
-4.0
-5.0
-6.0
0.0
1.5
3.0
G Low
G High
Tip displacement [nm]